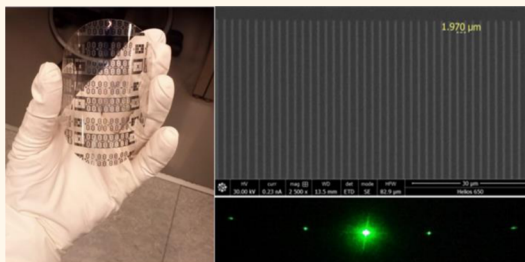


Focused Electron and Ion Beam Induced Deposition on Flexible and Transparent Polycarbonate Substrates

Patricia Peinado,[†] Soraya Sangiao,^{†,*§} and José M. De Teresa^{*,†,*,‡,⊥}

[†]Laboratorio de Microscopías Avanzadas (LMA), Instituto de Nanociencia de Aragón (INA), Universidad de Zaragoza, 50018 Zaragoza, Spain, [‡]Departamento de Física de la Materia Condensada, Universidad de Zaragoza, 50009 Zaragoza, Spain, [§]Fundación ARAID, 50018 Zaragoza, Spain, and [⊥]Instituto de Ciencia de Materiales de Aragón (ICMA), Universidad de Zaragoza—CSIC, 50009 Zaragoza, Spain

ABSTRACT The successful application of focused electron (and ion) beam induced deposition techniques for the growth of nanowires on flexible and transparent polycarbonate films is reported here. After minimization of charging effects in the substrate, sub-100 nm-wide Pt, W, and Co nanowires have been grown and their electrical conduction is similar compared to the use of standard Si-based substrates. Experiments where the substrate is bent in a controlled way indicate that the electrical conduction is stable up to high bending angles, $>50^\circ$, for low-resistivity Pt nanowires grown by the ion beam. On the other hand, the resistance of Pt nanowires grown by the electron beam changes significantly and reversibly with the bending angle. Aided by the substrate transparency, a diffraction grating in transmission mode has been built based on the growth of an array of Pt nanowires that shows sharp diffraction spots. The set of results supports the large potential of focused beam deposition as a high-resolution nanolithography technique on transparent and flexible substrates. The most promising applications are expected in flexible nano-optics and nanoplasmonics, flexible electronics, and nanosensing.



KEYWORDS: nanolithography · focused electron beam induced deposition · flexible transparent electronics · nanowires · diffraction gratings · magnetic materials · superconducting materials

Nanolithography comprises the set of techniques that allow the reduction of the dimensions of materials as well as the fabrication of nanodevices, generally through top-down techniques.¹ Some well-known examples of nanolithography techniques are optical lithography, electron-beam lithography, and nanoimprint lithography. Such techniques have recently been applied to the promising field of flexible electronics.^{2–10} Flexible electronics is a broad field in which electronic devices are built into flexible substrates for applications in low-cost microelectronics, portable biomedical applications, conformable chemical/physical sensors, lightweight displays and solar cells, etc. Within flexible electronics, transparent substrates are of special interest for applications in photonics and optoelectronics, giving rise to the subfield named *transparent flexible electronics (TFE)*. TFE is expected to reach applications in transparent electrodes for displays and photovoltaic or solar cells,^{11–13} wearable computers,¹⁴

smart contact lenses,¹⁵ etc. One of the remaining challenges in this field is to implement the existing general nanolithography techniques, which have been developed to meet the demands of standard Si-based semiconductor technology. However, difficulties arise due to issues such as chemical compatibility, substrate roughness, mechanical or thermal instabilities, and charging effects. In the present work, we demonstrate the feasibility of using focused electron and ion beam induced deposition (FEBID/FIBID) techniques to create functional (electrically and optically active) micro- and nanoscale patterns on transparent flexible polycarbonate substrates.

FEBID and FIBID are additive-lithography techniques where precursor molecules delivered by a gas-injection system become adsorbed onto a surface and are dissociated by a focused electron or ion beam, creating a local deposit. FEBID and FIBID permit high-resolution nanopatterning. In fact, by using a Pt metallorganic precursor, 3 nm Pt dots

* Address correspondence to deteresa@unizar.es.

Received for review March 4, 2015
and accepted June 2, 2015.

Published online June 02, 2015
10.1021/acsnano.5b01383

© 2015 American Chemical Society

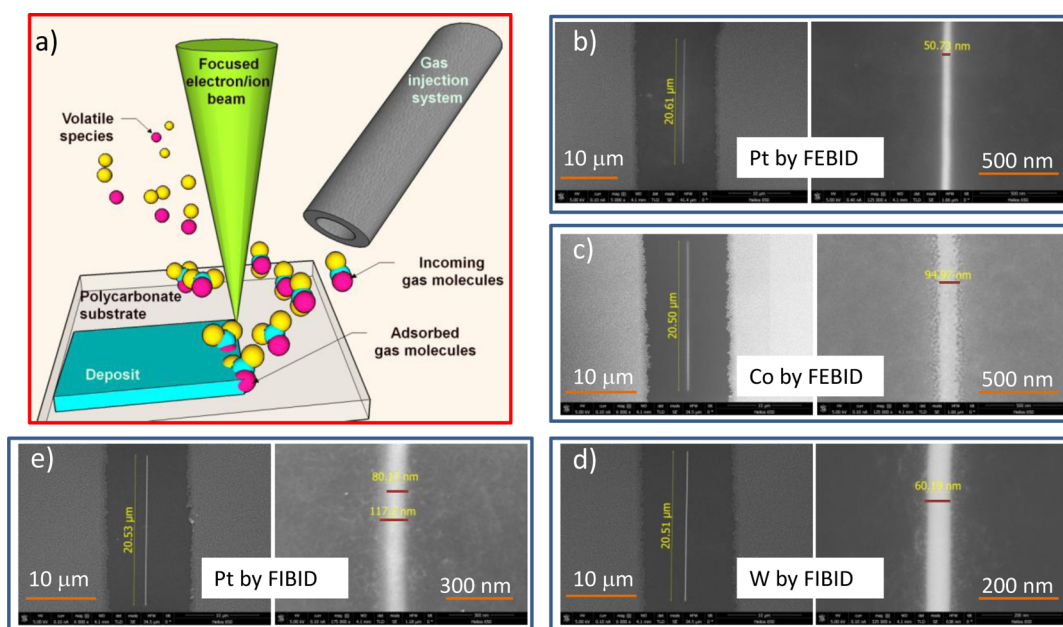


Figure 1. (a) Sketch showing the technique used to grow nanodeposits on flexible and transparent polycarbonate (PC) substrates. Scanning electron micrographs of the grown nanowires indicate the achievement of high lateral resolution: 50 nm for Pt nanowires by FEBID (b); 95 nm for Co nanowires by FEBID (c); 60 nm for W nanowires by FEBID (d); 80 nm for Pt nanowires by FIBID (e).

have been created with a scanning electron microscope on thin carbon membranes¹⁶ and Si substrates,¹⁷ and 10 nm-wide Pt nanowires have been grown with a focused ion beam.¹⁸ Besides the high resolution, FEBID and FIBID have additional advantages such as the capability to grow three-dimensional structures^{19,20} and their potential use on unconventional surfaces such as cantilever tips.^{21,22} However, the implementation of FEBID and FIBID techniques in flexible electronics for the fabrication of high-resolution nanodevices remains unexplored. Similarly, there is limited work on the use of these techniques for the fabrication of optical elements,^{23–25} and moreover, the use of flexible substrates can provide nanodevices with optical changes controlled by the substrate bending.^{26,27} In the present work, we challenge the growth of high-resolution functional materials by FEBID and FIBID on transparent and flexible substrates for potential use in TFE. Polycarbonate (PC) substrates have been chosen since they offer a number of advantages.²⁸ PC is a common engineering plastic used in multiple applications such as compact discs, lenses, cars, constructive parts, cell phone cases, etc. It shows good temperature resistance ($T_g = 147^\circ$), mechanical resistance, chemical resistance (to alcohols and diluted acids) and optical properties (almost transparent at wavelengths down to 400 nm). The transparency of PC, in combination with its lightweight compared to glass, has made it widely used in optical applications such as sunglasses, contact lenses, swimming goggles, automotive headlamps and windscreens in vehicles. Furthermore, the nanopatterning of PC substrates has allowed the exploration of some photonic applications of this

material. For example, Choi *et al.* have used an Atomic Force Microscope to pattern grating nanostructures on PC substrates,²⁹ while Burghoorn *et al.* have explored the nanopatterning of PC substrates by means of nanoimprint techniques for application as antireflective elements.³⁰ Given its physical and chemical properties as well as its broad range of applications, PC is an ideal candidate for TFE applications. Herein, we report that the nanopatterning of PC substrates by means of FEBID and FIBID techniques is feasible, allowing the exploration of interesting effects and devices.

RESULTS AND DISCUSSION

Growth of Nanowires on Polycarbonate Substrates. We have first addressed the feasibility of FEBID and FIBID growth on PC substrates. The following available precursor gas injection systems have been studied: $(\text{CH}_3)_3\text{Pt}(\text{CpCH}_3)$, $\text{W}(\text{CO})_6$, and $\text{Co}_2(\text{CO})_9$. In all cases, the main barrier to obtaining the desired deposits arises from charging effects occurring on the substrate. This type of problem is typical of insulating substrate materials due to the use of e^- in FEBID and Ga^+ in FIBID, but nevertheless can be managed in several ways. In our case, we have performed the growth close to metallic pads to allow easier charge evacuation. Once the charging effects are minimized, it is possible to target the growth of narrow structures, which is one of the main advantages of this technique. To obtain such high lateral resolution, it is necessary to use low beam currents, of the order of a few picoampere (pA), which have small beam spots. As can be noticed in Figure 1, it is possible to grow nanowires of aspect ratio >200 . The length of the nanowires has been fixed to

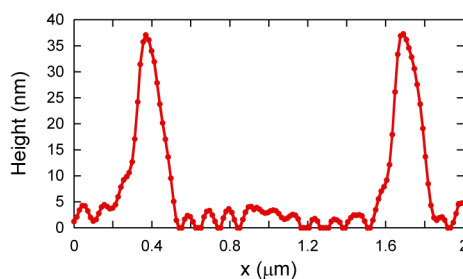
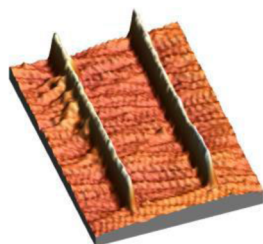
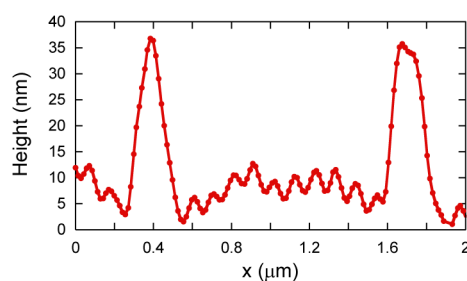
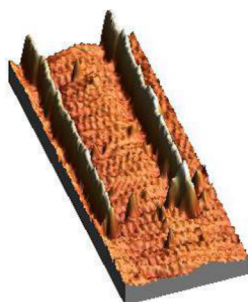
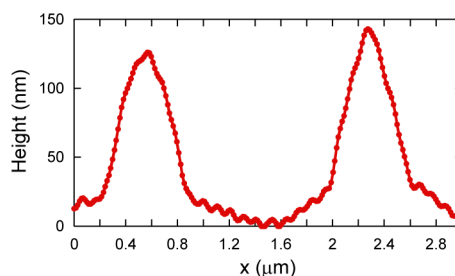
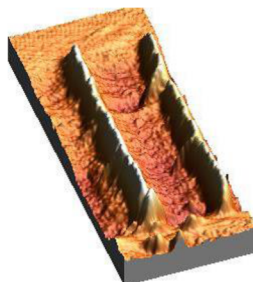
**Platinum
nanowires****Tungsten
nanowires****Cobalt
nanowires**

Figure 2. AFM measurements of some of the nanowires grown on the polycarbonate (PC) substrates: Pt by FEBID, W by FEBID, and Co by FEBID.

20 μm , and the width has been targeted to be as small as possible. The best results obtained after growth optimization are shown in Figure 1, with the corresponding widths of 50, 95, 60, and 80 nm, respectively, for deposits of Pt by FEBID, Co by FEBID, W by FIBID, and Pt by FEBID. The details about the growth of these nanowires are described in the Methods section. Figure 1 demonstrates that the use of FEBID and FIBID as nanolithography techniques on PC substrates is viable. Despite this, it is worth mentioning that the use of insulating substrates like PC is prone to charging effects and loss of lateral resolution of the grown deposits. This can be circumvented by some charge compensation strategy such as the use of an electron gun when depositing with the ion beam, adjustment of the working voltage, appropriate design of the metal structures around the FEBIP working area, and so forth.

We have selected three types of nanowires (Pt by FIBID, W by FIBID, Co by FEBID) to perform their topography characterization by atomic force microscopy (AFM). As shown in Figure 2, the polycarbonate substrate roughness is in the 5 nm range and shows some periodic structure of unknown origin.

The thickness of the nanowires can be very precisely determined with these measurements, but the apparent width observed in these measurements is determined by the convolution of the intrinsic nanowire width and the AFM tip dimensions. For that reason, the width is obtained from SEM images. The Pt, W, and Co nanowires are continuous and their roughness is comparable to that of the substrate.

Electrical Characterization of the Nanowires Grown on Polycarbonate Substrates. For many applications, one of the main issues of focused beam induced deposition techniques is the low metallic content and the corresponding high electrical resistivity.³¹ In the Methods section, data on the compositional study of the deposits can be found. These data indicate that the deposit composition is similar to the one measured in deposits grown on conventional substrates. To investigate the resistivity of the grown nanowires on PC substrates in comparison with the use of standard substrates (Si, SiO₂, etc.), we have first tackled the fabrication of metallic Al contact pads by optical lithography on the PC substrate. As described in the Methods section, some adjustments were required with respect to the

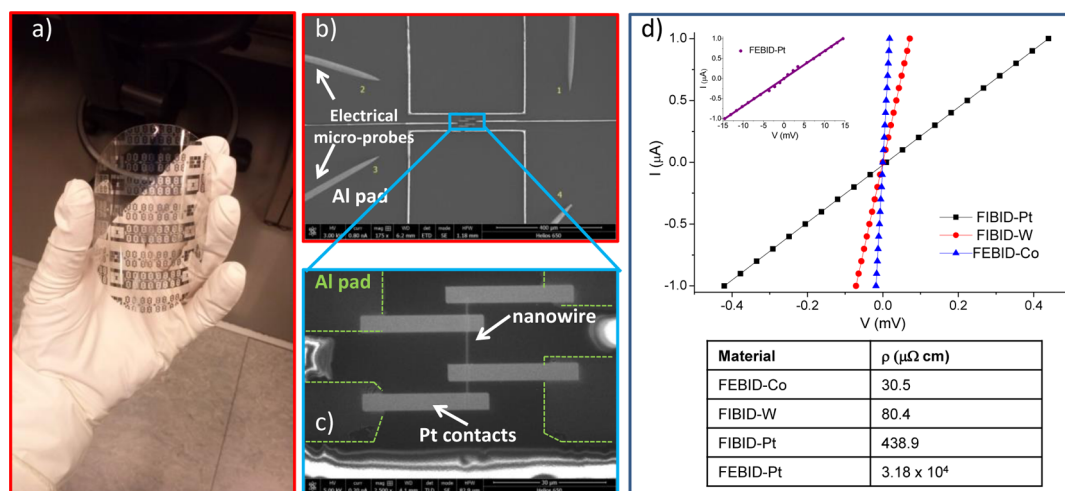


Figure 3. (a) Picture of a polycarbonate (PC) substrate patterned by means of optical lithography to allow electrical measurements. (b) Scanning electron micrographs of the patterned area of the polycarbonate substrate with Al pads together with microprobes ready for electrical measurements. (c) Scanning Electron micrographs of a typical grown nanowire and Pt contacts to permit the electrical measurements. (d) Electrical measurements (current *versus* voltage) of all the types of nanowires grown and the corresponding values of the resistivity obtained from such measurements and taking into account the dimensions of the nanowires.

standard process but there was no problem in generating clean Al contact pads, as shown in Figure 3. One of the properties of the PC substrate, its flexibility, is clearly observable in Figure 3a. The contact pads were designed to allow the growth of long nanowires (up to 50 μm or so) in the central part. To connect the nanowires to the Al contact pads, rectangular Pt deposits were grown by FEBID. The electrical resistivity measurements were performed using a microprobe station that allows precise location of the probes on the Al pads. Images of the probes are displayed in Figure 3b and of a typical nanowire in Figure 3c. Current-*versus*-voltage measurements of the following types of nanowires have been carried out to investigate their resistivity: Co by FEBID, W by FEBID, and Pt by FEBID and FIBID. The corresponding results are shown in Figure 3d. All the nanowires display linear current-*versus*-voltage in the voltage range studied and the absolute values of resistivity are similar or lower than those found using standard substrates. Thus, the most metallic nanowire is the Co one, with resistivity of 30.5 $\mu\Omega$ cm, similar to the value found by Fernández-Pacheco *et al.*³² Next, the W nanowire shows resistivity of 80.4 $\mu\Omega$ cm, similar to the value found by Li *et al.*³³ The Pt nanowire grown by FIBID presents a resistivity value of 438.9 $\mu\Omega$ cm, slightly lower than the previous value found by De Teresa *et al.*³¹ Similarly, the resistivity of the Pt nanowire grown by FEBID shows a resistivity value of 3.18×10^4 $\mu\Omega$ cm, lower than in our previous experiments using standard silicon oxide substrates.³¹ Such improvement likely arises from a minimized carbon contamination of the deposit in the present case due to improved vacuum conditions in the growth chamber used in the present study. Summarizing, the use of PC substrates maintains the

electrical properties of the grown nanowires, not hampering their applicability. More specifically, the W deposits grown by FIBID can be used for circuit editing and mask repair,³⁴ for electrical contacting of nanostructures,³⁵ and in superconductivity studies below 5 K.^{36–38} The Pt deposits grown by FEBID and FIBID can be used for electrical contacting of nanostructures,^{39,40} being particularly successful when applied to semiconducting nanowires for gas sensing.⁴¹ The Co nanowires are being studied for their potential applicability in magnetic storage, logic, and sensing.⁴²

One of the main potential advantages of the PC substrate is its bendability. A mechanical device has been constructed to perform systematic measurements of the electrical resistance of the grown nanowires as a function of the bending angle. The results are shown in Figure 4a, using a Pt nanowire grown by FIBID (ion voltage of 30 kV and ion current of 7 pA) with the following dimensions: length = 30 μm , width = 160 nm, thickness = 100 nm. With the use of electrical microprobes, the electrical resistance was monitored as a function of the bending angle for a few bending angles. The electrical resistance remained constant (within the noise below 1%) up to a high bending angle, 52.3°, in which the electrical resistance increased by a factor of 500, probably due to the appearance of some cracking in the nanowire. The robustness of the electrical resistance of these nanowires against bending underlines their potential use in applications where the substrate is flexible and the resistance of the nanowire needs to remain unchanged.^{2–15}

Importantly, the electrical resistance of deposits grown by FEBID can be very sensitive to mechanical deformations⁴³ or variation in humidity.⁴⁴ Thus, such

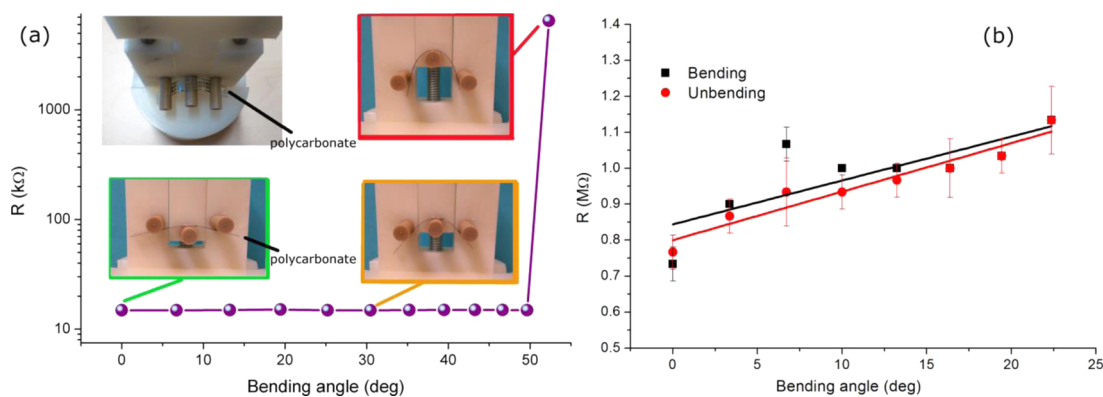


Figure 4. (a) Measurements of the electrical resistance of a Pt nanowire grown by FEBID as a function of the bending angle of the polycarbonate substrate. Images of the substrate bending along such measurements are also shown. (b) Similar measurements for a Pt nanowire grown by FEBID for bending as well as unbending of the substrate.

type of deposits could eventually bear the information on the mechanical deformation or the humidity environment that the device is submitted to, expanding the applicability of nanodeposits grown on PC substrates. To explore such possibility, Pt nanowires were grown by FEBID and their resistance was measured against substrate bending. The results are shown in Figure 4b. In this case, the substrate bending provoked a significant change of the nanowire resistance, which returned to the original value after unbending. This effect can be explained by the microstructure of the nanowires, which is composed by small Pt grains (about 3 nm in diameter) immersed in a carbonaceous matrix. The conduction mechanism is through tunneling between the neighboring Pt nanoparticles and, as a consequence, is very sensitive to changes in the average distance between them.⁴³ In the present case, the bending of the substrate produces an elongation of the nanowire along its long axis that increases the distance between the Pt nanoparticles, resulting in the resistance augmentation. In the case of the nanowires grown by FEBID, shown in Figure 4a, such variation of the resistance against bending is not observed because the conduction mechanism is different, as evidenced by the absolute value of the resistivity, a factor of 100 smaller than in the case of Pt nanowires grown by FEBID. For Pt nanowires grown by FEBID, the value of resistivity is typical of a dirty metal, indicating that the Pt grains are mainly connected and the primary conduction mechanism is not through tunneling.³¹

After demonstrating the potential for growing flexible electronic nanowires by focused beam deposition on PC substrates, we decided to explore their applicability in nano-optics, taking advantage of the transparent nature of the substrate. The transparency of the PC substrates adds optical functionality in transmission mode, which is explored hereafter through the fabrication of a diffraction grating based on Pt nanowires grown by FEBID. To the best of our knowledge, these results constitute the first experimental evidence of the use of focused beam induced deposition techniques

for application in diffraction gratings. Diffraction gratings are commonly used in classical applications such as instrumental analysis, laser systems and astronomical telescopes as well as in more recent applications like fiber-optic telecommunications, beam splitters, optical couplers and metrology.⁴⁵ We have designed the most appropriate nanowire array for the subsequent optical experiment, displayed in Figure 5. The experiment consists of the laser illumination of the nanowire array grown on the transparent PC substrate, which diffracts the incident light. The diffraction pattern thus obtained is collected on a screen placed behind the substrate, where the expression for the position of the diffraction maxima when the incident light is perpendicular to the substrate is given by eq 1:

$$\sin\Theta_n = \frac{n\lambda}{d} \quad (1)$$

where λ is the light wavelength (here 532 nm, provided by a laser), d is the nanowire periodicity (in this case 1.97 μm , as shown in Figure 5), n is the diffraction order, and Θ_n is the diffraction angle corresponding to the n diffraction order. The calculated first and second diffraction spots should appear at 15.7° and 32.7° and the experimental values are close to such values: 15.9° and 33.8°. This is a simple but clarifying experiment of the potentiality of FEBID and FIBID on transparent substrates for optical applications, which remains basically unexplored. It is worth mentioning that a large number of micro- and nano-optical devices are investigated for future technology and their functionality lies at a large extent on the precise micro- and nano- dimensions of the active optical element.⁴⁶ Laser writing⁴⁷ and electron beam lithography^{48,49} are frequently used to obtain the required patterns in such applications. However, such techniques have some limitations in resolution or processing and focused beam induced deposition could be an alternative technology with the aforementioned advantages of being single step and having high resolution, 3D capabilities and growth on arbitrary substrate. In fact, FEBID techniques have been

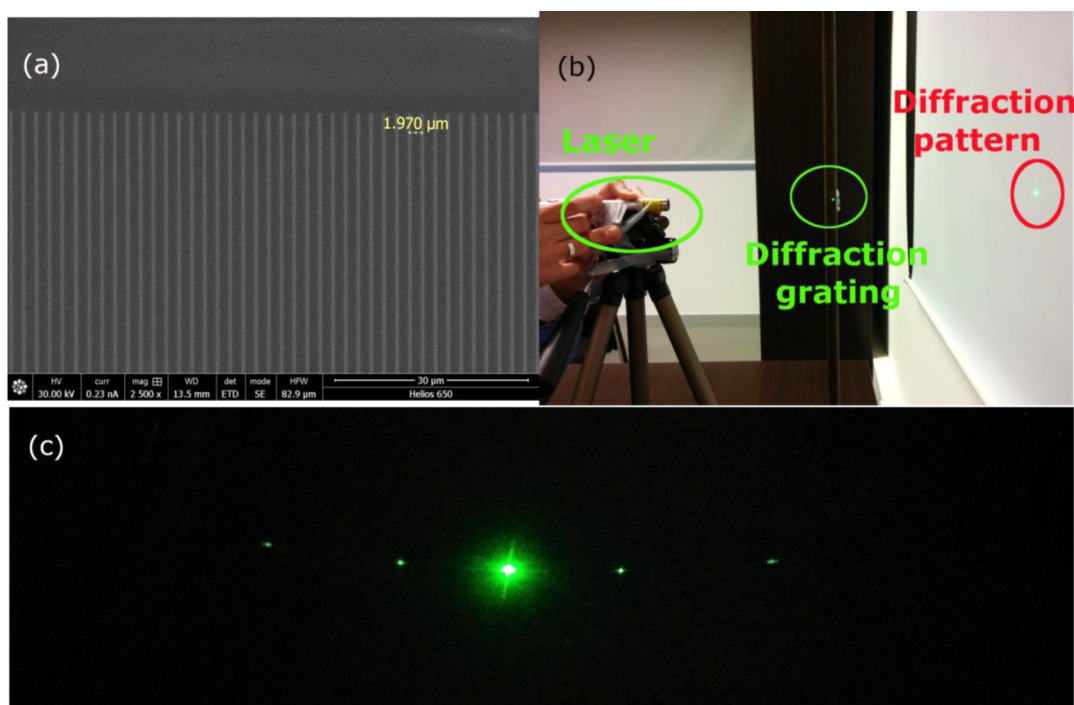


Figure 5. (a) Diffraction grating formed by Pt wires grown by FIBID on polycarbonate (PC) substrates. (b) Experimental setup for the measurement of the diffraction pattern in transmission mode created by such grating. (c) Zoom-in of the diffraction pattern generated in the experiment shown in (b). As described in the text, the diffraction spots are located at the expected positions given the light incidence angle (perpendicular to the substrate), the laser wavelength (532 nm) and the nanowire periodicity (1.97 μm).

used to fabricate nano-optical structures based on Au or Pt deposits^{20,23,25} or as nanomasks for subsequent gold evaporation.⁵⁰ The combination of those and other types of optically active structures with flexible and transparent substrates is consequently perceived as a promising future research field.

CONCLUSIONS

The present results indicate that FEBID and FIBID techniques are viable additive nanolithography techniques to pattern flexible transparent substrates such as polycarbonate films. This opens new perspectives in the extension of the applicability of these powerful nanolithography techniques. On top of the known general advantages of FEBID and FIBID (single-step process, high resolution, 3D capabilities), the use of flexible transparent substrates permits their application in flexible electronics as well as in nano-optics and optoelectronics. In the field of flexible electronics, the most promising applications could be found in the fabrication of flexible nanoscale sensors which are

robust against substrate bending for applications such as monitoring of temperature, specific gas, humidity, magnetism, *etc.*^{41–44} Moreover, specific nanodeposits can be designed to measure the substrate bending itself due to their increase of electrical resistance with the bending angle. The substrate transparency will be suitable for fabricating not only diffraction gratings (as shown here) but also other optical elements such as optical waveguides, couplers, Fresnel lenses, sensors, *etc.* In particular, the most promising applications could occur in the emerging field of nanoplasmonics thanks to the combination of the high resolution in the fabrication of the nanostructures by FEBID and FIBID and the use of gold or silver precursors. Finally, it is also worth mentioning that the use of magnetic or superconducting deposits on transparent substrates will allow the exploration of advanced magneto-optical or superconductive-optical effects. In summary, the use of nanolithography techniques based on FEBID and FIBID on flexible transparent substrates provides new degrees of freedom in the fabrication of nanodevices in multiple fields.

METHODS

Patterning of Polycarbonate Substrates by Optical Lithography. Polycarbonate sheets (LEXAN) of 127 μm thickness were purchased from Tizaro (code LEXAN GRA0713001007). The patterning of a 3-in. polycarbonate wafer with optical lithography began with the evaporation of 50 nm of aluminum. After designing a

suitable optical mask for the electrical transport experiments, a positive photoresist (A6632) was spun on the wafer, UV exposed with a MA/BA 6 Mask Aligner by Süss Microtec, and developed with a diluted sodium-based developer. Then, a concentrated solution of the developer was used to produce wet etching of the Al not covered with the photoresist. Ultrasonic baths were used to speed up the process.

Growth Parameters of the Nanowires. The nanowires shown in Figure 1 were synthesized as follows. In general, the current was in the pA range to guarantee the growth of narrow structures, whereas the voltage was chosen either to minimize charging effects, maximize the nanowire metal content, or enhance the lateral resolution. The FIBID Pt nanowires were grown under 30 kV beam voltage. Along several optimization experiments, the ion beam current was progressively diminished, starting in the nanoampere (nA) range and finishing in the pA range (7.7 pA). Under such low current, high lateral resolution (125 nm) was obtained. The FEBID Pt nanowires were grown under 5 kV electron beam voltage. With the use of an electron beam current of 1.6 nA, it was possible to achieve high lateral resolution (50 nm). The FIBID W nanowires were grown under 30 kV ion beam voltage. Along several optimization experiments, the ion beam current was progressively diminished to reach high lateral resolution (<100 nm) when the ion beam current was 24 pA. The FEBID Co nanowires were grown under 5 kV electron beam voltage and electron beam current of 1.6 nA, reaching high lateral resolution (<100 nm). The nanowires used in the electrical transport experiments shown in Figure 3 were prepared using the optimized growth conditions: 30 kV/7.7 pA for the FIBID Pt nanowires, 5 kV/1.6 nA for the FEBID Pt nanowires, 30 kV/24 pA for the FIBID W nanowires, and 5 kV/1.6 nA for the FEBID Co nanowires. The most straightforward way to measure the width of the nanowires was through the white/black change of contrast observed in the SEM micrographs with top-down view. In some nanowires, we cross-checked the obtained value with cross-sectional SEM images taken in the standard way (deposit coverage, FIB cut and SEM inspection). Both methods were found to provide similar values of the width. We would like to point out that we want to provide the typical values of width obtained and are not interested in giving very accurate values for each individual nanowire.

Compositional Study by Means of EDS. We have studied the metal content of three types of nanodeposits (Pt by FIBID, W by FIBID, Co by FEBID) by Energy Dispersive X-ray Spectroscopy (EDS) to check that the metal content is similar to that obtained in deposits grown on standard substrates such as silicon ones. The voltage used in the EDS experiments was 5 kV. To get enough signal, the deposits were grown with dimensions 500 nm × 500 nm × 100 nm. The respective growth conditions were as follows:

- Pt by FIBID: voltage of 30 kV and current of 7 pA
- W by FIBID: voltage of 30 kV and current of 18 pA
- Co by FEBID: voltage of 5 kV and current of 1.6 nA

The metal content (atomic percent) in the case of the Pt deposit was 32%, similar to the value obtained when standard Si substrates are used.³¹ The metal content in the case of the W deposit was 63%, also similar to the value obtained when standard Si substrates are used.⁵¹ The metal content in the case of the Co deposit was 84%, slightly smaller than the value obtained when standard Si substrates are used (90%).³² In this case, the measured C content is 11%, whereas the O content is 5%, which points to signal contamination from the electrons penetrating into the substrate instead of lack of Co₂(CO)₈ precursor dissociation. The low resistivity value of the Co nanowires shown in the main text is also a good hallmark of the high Co content of deposits on polycarbonate substrates.

AFM Experiments. These experiments were carried out with a commercial VEECO Multimode 8 system using noncontact mode. We selected three types of nanowires (Pt by FIBID, W by FIBID, Co by FEBID) to perform their topography characterization by Atomic Force Microscopy (AFM). The growth conditions in each case were as follows:

- Pt by FIBID: voltage of 30 kV and current of 0.79 nA
- W by FIBID: voltage of 30 kV and current of 33 pA
- Co by FEBID: voltage of 5 kV and current of 1.6 nA

Geometry of the Nanowires Measured in Figure 3. Using the following nomenclature, L = length, W = width, t = thickness, the dimensions of the studied nanowires were as follows. FEBID-Co: $L = 9.5 \mu\text{m}$, $W = 1.6 \mu\text{m}$, $t = 100 \text{ nm}$; FIBID-W: $L = 8.97 \mu\text{m}$, $W = 1.01 \mu\text{m}$, $t = 100 \text{ nm}$; FIBID-Pt: $L = 8.03 \mu\text{m}$, $W = 160.2 \text{ nm}$, $t = 100 \text{ nm}$; FEBID-Pt: $L = 8.36 \mu\text{m}$, $W = 1.84 \mu\text{m}$, $t = 100 \text{ nm}$

Conflict of Interest: The authors declare no competing financial interest.

Acknowledgment. This work was supported by Spanish Ministry of Economy and Competitiveness through projects No. MAT2011-27553-C02 and MAT2014-51982-C2-1-R including FEDER funds and by the Aragon Regional Government. Help by L. Casado in the growth experiments, by J. Michalik in the electrical measurements, by J. L. Díez in the AFM experiments and by S. Mitchell in the manuscript polishing are warmly acknowledged. J.M.D.T. proposed the experiments, supervised the research, and wrote the manuscript. P.P. and S.S. performed the experiments, contributed to the manuscript, and have given approval to the final version of the manuscript.

REFERENCES AND NOTES

- Xia, Y. N.; Rogers, J. A.; Paul, K. E.; Whitesides, J. M. Unconventional Methods for Fabricating and Patterning Nanostructures. *Chem. Rev.* **1999**, *99*, 1823–1848.
- Forrest, S. R. The Path to Ubiquitous and Low-Cost Organic Electronic Appliances on Plastic. *Nature* **2004**, *428*, 911–918.
- Ishikawa, F. N.; Chang, H.-K.; Ryu, K.; Chen, P.; Badmaev, A.; Gomez de Arco, L.; Shen, G.; Zhou, C. Transparent Electronics Based on Transfer Printed Aligned Carbon Nanotubes on Rigid and Flexible Substrates. *ACS Nano* **2009**, *3*, 73–79.
- Melzer, M.; Makarov, D.; Calvimontes, A.; Karnaushenko, D.; Baunack, S.; Kaltofen, R.; Mei, Y.; Schmidt, O. G. Stretchable Magneto-electronics. *Nano Lett.* **2011**, *11*, 2522.
- Artukovic, A.; Kaempgen, M.; Hecht, D. S.; Roth, S.; Grüner, G. Transparent and Flexible Carbon Nanotube Transistors. *Nano Lett.* **2005**, *5*, 757–760.
- Lee, C. H.; Kim, D. R.; Zheng, X. Fabrication of Nanowire Electronics on Nonconventional Substrates by Water-Assisted Transfer Printing Method. *Nano Lett.* **2011**, *11*, 3435–3439.
- Bedoya-Pinto, A.; Donolato, M.; Gobbi, M.; Hueso, L.; Vavassori, P. Flexible Electronic Devices on Kapton. *Appl. Phys. Lett.* **2014**, *104*, 062412.
- Sun, Y. G.; Rogers, J. A. Inorganic Semiconductors for Flexible Electronics. *Adv. Mater.* **2007**, *19*, 1897–1916.
- Withers, F.; Bointon, T. H.; Dubois, M.; Russo, S.; Craciun, M. F. Nanopatterning of Fluorinated Graphene by Electron Beam Irradiation. *Nano Lett.* **2011**, *11*, 3912–3916.
- Park, I.; Ko, S. H.; Pan, H.; Grigoropoulos, C. P.; Pisano, A. P.; Fréchet, J. M. J.; Lee, E.-S.; Jeong, J.-H. Nanoscale Patterning and Electronics on Flexible Substrate by Direct Nanoimprint of Metallic Nanoparticles. *Adv. Mater.* **2008**, *20*, 489–496.
- Hu, L.; Kim, H. S.; Lee, J.-Y.; Peumans, P.; Cui, Y. Scalable Coating and Properties of Transparent Flexible, Silver Nanowire Electrodes. *ACS Nano* **2010**, *4*, 2955–2963.
- Kim, K. S.; Zhao, Y.; Jang, H.; Lee, S. Y.; Kim, J. M.; Kim, K. S.; Ahn, J.-H.; Kim, P.; Choi, J.-Y.; Hong, B. H. Large-Scale Pattern Growth of Graphene Films for Stretchable Transparent Electrodes. *Nature* **2009**, *457*, 706–710.
- Ju, S.; Facchetti, A.; Suan, Y.; Liu, J.; Ishikawa, F.; Ye, P.; Zhou, C.; Marks, T. J.; Janes, D. B. Fabrication of Fully Transparent Nanowire Transistors for Transparent and Flexible Electronics. *Nat. Nanotechnol.* **2007**, *2*, 378–384.
- Nomura, K.; Ohta, H.; Takagi, A.; Kamiya, T.; Hirano, M.; Hosono, H. Room-Temperature fabrication of Transparent Flexible Thin-Film Transistors Using Amorphous Oxide Semiconductors. *Nature* **2004**, *432*, 488.
- Salvatore, G. A.; Mützenrieder, N.; Kinkeldei, T.; Petti, L.; Zysset, C.; Strebler, I.; Büthe, L.; Tröster, G. Wafer-Scale Design of Lightweight and Transparent Electronics that Wraps around Hairs. *Nat. Commun.* **2014**, *5*, 2982.
- van Kouwen, L.; Botman, A.; Hagen, C. W. Focused Electron-Beam-Induced Deposition of 3 nm Dots in a Scanning Electron Microscope. *Nano Lett.* **2009**, *9*, 2149–2152.
- van Oven, J. C.; Berwald, F.; Berggren, K. K.; Kruit, P.; Hagen, C. W. Electron-Beam-Induced Deposition of 3-nm-Half-Pitch Patterns on Bulk Si. *J. Sci. Vac. Technol., B* **2011**, *29*, 06F305.
- Maas, D. J.; van der Drift, E. W.; van Veldhoven, E.; Moessen, J.; Rudneva, M.; Alkemade, P. F. A. Nano-Engineering with a

- Focused Helium Ion Beam. *Mater. Res. Soc. Symp. Proc.* **2011**, *1354*, 33–46.
19. Bøggild, P.; Hansen, T. M.; Tanasa, C.; Grey, F. Fabrication and Actuation of Customized Nanotweezers with a 25 nm Gap. *Nanotechnology* **2001**, *12*, 331–335.
 20. Höflich, K.; Yang, R. B.; Berger, A.; Leuchs, G.; Christiansen, S. The Direct Writing of Plasmonic Gold Nanostructures by Electron-Beam-Induced Deposition. *Adv. Mater.* **2011**, *23*, 2657–2661.
 21. Utke, I.; Hoffmann, P.; Berger, R.; Scandella, L. High-Resolution Magnetic Co Supertips Grown by a Focused Electron Beam. *Appl. Phys. Lett.* **2002**, *80*, 4792–4794.
 22. Lavenant, H.; Naletov, V. V.; Klein, O.; de Loubens, G.; Casado, L.; De Teresa, J. M. Mechanical Magnetometry of Cobalt Nanospheres deposited by Focused Electron Beam at the Tip of Ultra-Soft Cantilevers. *Nanofabrication* **2014**, *1*, 65–73.
 23. Graells, S.; Acimovic, S.; Volpe, G.; Quidant, R. Direct Growth of Optical Antennas Using E-Beam-Induced Gold Deposition. *Plasmonics* **2010**, *5*, 135–139.
 24. Makise, K.; Mitsuishi, K.; Shimajo, M.; Furuya, K. A Nano-sized Photodetector Fabricated by Electron-Beam-Induced Deposition. *Nanotechnology* **2009**, *20*, 425305.
 25. Esposito, M.; Tasco, V.; Todisco, F.; Cuscunà, M.; Benedetti, A.; Sanvitto, D.; Passaseo, A. Triple-Helical Nanowires by Tomographic Rotatory Growth for Chiral Photonics. *Nat. Commun.* **2015**, *6*, 6484.
 26. Aksu, S.; Huang, M.; Artar, A.; Yanik, A.; Selvarasah, S.; Dokmeci, M.; Altug, H. Flexible Plasmonics on Unconventional and Nonplanar Substrates. *Adv. Mater.* **2011**, *23*, 4422–4430.
 27. Hu, J.; Li, L.; Lin, H.; Zhang, P.; Zhou, W.; Ma, Z. Flexible Integrated Photonics: Where Materials, Mechanics and Optics Meet. *Opt. Mater. Express* **2013**, *3*, 1313–1331.
 28. City Plastics, Description of Polycarbonate material, <http://www.cityplastics.com.au/materials-polycarbonate/> (accessed Jan 2015).
 29. Choi, C. H.; Lee, D. J.; Sung, J.-H.; Lee, M. W.; Lee, S.-G.; Park, S.-G.; Lee, E.-H.; O, B.-H. A Study of AFM-Based Scratch Process on Polycarbonate Surface and Grating Applications. *Appl. Surf. Sci.* **2010**, *256*, 7668–7671.
 30. Burghoorn, M.; Roosen-Melsen, D.; de Riet, J.; Sabik, S.; Vroon, Z.; Yakimets, I.; Buskens, P. Single Layer Broadband Anti-Reflective Coatings for Plastic Substrates Produced by Full Wafer and Roll-to-Roll Step-and-Flash Nano-Imprint Lithography. *Materials* **2013**, *6*, 3710–3726.
 31. De Teresa, J. M.; Córdoba, R.; Fernández-Pacheco, A.; Montero, O.; Strichovanec, P.; Ibarra, M. R. Origin of the Difference in the Resistivity of As-Grown Focused-Ion- and Electron-Beam-Induced Pt Nanodeposits. *J. Nanomater.* **2009**, *2009*, 936863.
 32. Fernández-Pacheco, A.; De Teresa, J. M.; Córdoba, R.; Ibarra, M. R. High-Quality Magnetic and Transport Properties of Cobalt Nanowires Grown by Focused-Electron-Beam-Induced Deposition. *J. Phys. D: Appl. Phys.* **2009**, *42*, 055005.
 33. Li, W.; Fenton, J. C.; Wang, Y.; McComb, D. W.; Warburton, P. A. Tunability of the Superconductivity of Tungsten Films Grown by Focused-Ion-Beam Direct Writing. *J. Appl. Phys.* **2008**, *104*, 093913.
 34. Stewart, D. K.; Stern, L. A.; Morgan, J. C. Focused-Ion-Beam Induced Deposition of Metal for Microcircuit Modification. *SPIE Proc.* **1989**, *1089*, 18.
 35. Marcano, N.; Sangiao, S.; Plaza, M.; Pérez, L.; Fernández-Pacheco, A.; Córdoba, R.; Sánchez, M. C.; Morellón, L.; Ibarra, M. R.; De Teresa, J. M. Weak Antilocalization Signatures in the Magnetotransport Properties of Individual Electrodeposited Bi Nanowires. *Appl. Phys. Lett.* **2010**, *96*, 082110.
 36. Shailos, A.; Nativel, W.; Kasumov, A.; Collet, C.; Ferrier, M.; Guéron, S.; Deblock, R.; Bouchiat, H. Proximity Effect and Multiple Andreev Reflection in Few-Layer Graphene. *EPL* **2007**, *79*, 57008.
 37. Romans, E. J.; Osley, E. J.; Young, L.; Warburton, P. A.; Li, W. Three-Dimensional Nanoscale Superconducting Quantum Interference Device Pickup Loops. *Appl. Phys. Lett.* **2010**, *97*, 222506.
 38. Córdoba, R.; Baturina, T. I.; Sesé, J.; Mironov, A. Y.; De Teresa, J. M.; Ibarra, M. R.; Nasimov, D. A.; Gutakovskii, A. K.; Latyshev, A. V.; Guillamón, I.; et al. Magnetic Field Induced Dissipation Free State in Superconducting Nanostructures. *Nat. Commun.* **2013**, *4*, 1437.
 39. Cronin, S. B.; Lin, Y.-M.; Rabin, O.; Black, M. R.; Ying, J. Y.; Dresselhaus, M. S.; Gai, P. L.; Minet, J.-P.; Issi, J.-P. Making Electrical Contacts to Nanowires with a Thick Oxide Coating. *Nanotechnology* **2002**, *13*, 653–658.
 40. Gopal, V.; Radmilovic, V. R.; Daraiao, C.; Yin, S.; Yang, P.; Stach, E. A. Rapid Prototyping of Site-Specific Nanocontacts by Electron and Ion Beam Assisted Direct-Write Nanolithography. *Nano Lett.* **2004**, *4*, 2059–2063.
 41. Hernández-Ramírez, F.; Prades, J. D.; Tarancón, A.; Barth, S.; Casals, O.; Jiménez-Díaz, R.; Pellicer, E.; Rodríguez, J.; Juli, M. A.; Romano-Rodríguez, A.; et al. Portable Microsensors Based on Individual SnO₂ Nanowires. *Nanotechnology* **2007**, *18*, 495501.
 42. De Teresa, J. M.; Fernández-Pacheco, A. Present and Future Applications of Magnetic Nanostructures Grown by FEBID. *Appl. Phys. A: Mater. Sci. Process.* **2014**, *117*, 1645.
 43. Schwalb, C. H.; Grimm, C.; Baranowski, M.; Sachser, R.; Porrati, F.; Reith, H.; Das, P.; Müller, J.; Völklein, F.; Kaya, A.; et al. A tunable Strain Sensor Using Nanogranular Material. *Sensors* **2010**, *10*, 9847–9856.
 44. Kolb, F.; Grimm, C.; Schmoltner, K.; Huth, M.; Hohenau, A.; Krenn, J.; Klug, A.; List, E. J. W.; Plank, H. Variable Tunnel Barriers in FEBID Based PtC Metal-Matrix Nanocomposites as a Transducing Element for Humidity Sensing. *Nanotechnology* **2013**, *24*, 305501.
 45. Lal, S.; Link, S.; Halas, N. J. Nano-Optics from Sensing to Waveguiding. *Nat. Photonics* **2007**, *1*, 641–648.
 46. Palmer, C. *Diffraction Grating Handbook*, 7th ed.; Richardson Gratings: Rochester, NY, 2014.
 47. Gale, M. T.; Rossi, M.; Pedersen, J.; Schütz, H. Fabrication of Continuous-Relief Micro-Optical Elements by Direct Laser Writing in Photoresists. *Opt. Eng.* **1994**, *33*, 3556–3566.
 48. Di Fabrizio, E.; Romanato, F.; Gentili, M.; Cabrini, S.; Kaulich, B.; Susini, J.; Barrett, R. High-Efficiency Multilevel Zone Plates for Kev X-rays. *Nature* **1999**, *401*, 895–898.
 49. Sarov, Y.; Kostic, I.; Hrkut, P.; Matay, L.; Ivanov, T. Z.; Rangelow, I. Fabrication of Diffraction Gratings for Microfluidic Analysis. *Bulg. J. Phys.* **2002**, *29*, 17–29.
 50. Schuck, P. J.; Weber-Bargioni, A.; Ashby, P. D.; Ogletree, D. F.; Schwartzberg, A.; Cabrini, S. Life Beyond Diffraction: Opening New Routes to Materials Characterization with Next-Generation Optical Near-Field Approaches. *Adv. Funct. Mater.* **2013**, *23*, 2539–2553.
 51. Guillamón, I.; Suderow, H.; Vieira, S.; Fernández-Pacheco, A.; Sesé, J.; Córdoba, R.; De Teresa, J. M.; Ibarra, M. R. Nanoscale Superconducting Properties of Amorphous W-Based Deposits Grown with Focused Ion Beam. *New J. Phys.* **2008**, *10*, 093005.